Langmuir
Article
pubs.acs.org/Langmuir

Multifunctional Superparamagnetic Janus Particles

Kai P. Yuet, Dae Kun Hwang, Ramin Haghgooie, and Patrick S. Doyle*

Department of Chemical Engineering, Massachusetts Institute of Technology, Cambridge, Massachusetts, 02139

Received September 7, 2009. Revised Manuscript Received October 6, 2009

In this study, we report the microfluidic-based synthesis of a multifunctional Janus hydrogel particle with anisotropic superparamagnetic properties and chemical composition for the bottom-up assembly of hydrogel superstructures. In a uniform magnetic field, the resulting Janus magnetic particles fabricated in the present method exhibit chainlike or meshlike superstructure forms, the complexity of which can be simply modulated by particle density and composition. This controllable field-driven assembly of the particles can be potentially used as building blocks to construct targeted superstructures for tissue engineering. More importantly, we demonstrated that this method also shows the ability to generate multifunctional Janus particles with great design flexibilities: (a) direct encapsulation and precise spatial distribution of biological substance and (b) selective surface functionalization in a particle. Although these monodisperse particles find immediate use in tissue engineering, their ability to self-assemble with tunable anisotropic configurations makes them an intriguing material for several exciting areas of research such as photonic crystals, novel microelectronic architecture, and sensing.

1. Introduction

Recently, advances in three-dimensional hydrogels have generated microstructures that successfully simulate native cellular microenvironments with regards to optimal mechanical behavior as well as growth factor and nutrient delivery.[1] Hydrogels—hydrated hydrophilic polymer networks with finely tunable biocompatibility, mechanical stability, degradability, shape, and composition—are widely used as tissue engineering scaffolds,[2] environmentally responsive drug delivery systems,[3] and critical components in diagnostic devices.[4] Despite its promise in many tissue engineering and regenerative medicine applications, hydrogel technology falls short of reconstructing the intricacies of physiological structures such as organs and vascularized tissues.[1] "Bottom-up" assembly approaches attempt to replicate nature's use of repeating structures to build constructs by assembling well-characterized building blocks.[5,6] However, implementations of bottom-up assembly of hydrogels have been limited to random packing processes,[7] microfluidic guidance,[8] physical manipulation,[9] or a combination of mechanical agitation and hydrophobic assembly,[10] constraining the complexity and scalability of the resulting constructs. In particular, magnetic interactions are widely utilized to assemble magnetic nanoparticles into chains,[11] two-dimensional[12] and three-dimensional aggregates,[13] and even highly ordered structures such as nanocrystal superlattices[14] and photonic colloidal crystals,[15] though their role in hydrogel self-assembly have remained largely unexplored. Therefore, potential strategies such as field-driven assembly that easily generate complex hydrogel architecture can accelerate efforts to develop biomimetic tissues of organs for replacement, repair, or transplantation.

Anisotropic particles are potentially powerful building blocks for constructing complicated targeted structures because of their peculiar shapes and interactions.[6] In particular, Janus particles[16,17]—zero-dimensional particles with dual functionalities arising from chemically heterogeneous phases—are attracting much attention because of their potential applications in electronic paper,[18] photonic materials,[19] emulsion stabilization,[17] imaging probes,[20] and sensors.[19] Generally, Janus particles are synthesized by either direct (dual-supplied) droplet formation or indirect chemical or physical modification techniques (toposelective surface modification).[17] Direct dual-supplied methods require the breakup of two parallel coflowing streams of polymeric solutions in microfluidic devices,[18,19,21,22] electrified jetting,[20] or spinning disks;[17] however, toxic immiscible and/or viscous monomer or polymer solutions are typically used to preserve sharp interfaces for Janus particle production.[18−21] Alternatively, toposelective surface or template-directed modification methods require the embedding of

* Address correspondence to pdoyle@mit.edu.

(1) Khademhosseini, A.; Langer, R.; Borenstein, J.; Vacanti, J. P. *Proc. Natl. Acad. Sci. U.S.A.* **2006**, *103*, 2480–2487.
(2) Cushing, M. C.; Anseth, K. S. *Science* **2007**, *316*, 1133–1134.
(3) Qiu, Y.; Park, K. *Adv. Drug Delivery Rev.* **2001**, *53*, 321–339.
(4) Pregibon, D. C.; Toner, M.; Doyle, P. S. *Science* **2007**, *315*, 1393–1396.
(5) Whitesides, G. M.; Grzybowski, B. *Science* **2002**, *295*, 2418–2421.
(6) Glotzer, S. C.; Solomon, M. J. *Nat. Mater.* **2007**, *6*, 557–562.
(7) McGuigan, A. P.; Sefton, M. V. *Proc. Natl. Acad. Sci. U.S.A.* **2006**, *103*, 11461–11466.
(8) Chung, S. E.; Park, W.; Shin, S.; Lee, S. A.; Kwon, S. *Nat. Mater.* **2008**, *7*, 581–587.
(9) Yeh, J.; Ling, Y.; Karp, J. M.; Gantz, J.; Chandawarkar, A.; Eng, G.; Blumling, r., J.; Langer, R.; Khademhosseini, A. *Biomaterials* **2006**, *27*, 5391–5398.
(10) Du, Y.; Lo, E.; Ali, S.; Khademhosseini, A. *Proc. Natl. Acad. Sci. U.S.A.* **2008**, *105*, 9522–9527.
(11) Tanase, M.; Bauer, L. A.; Hultgren, A.; Silevitch, D. M.; Sun, L.; Reich, D. H.; Searson, P. C.; Meyer, G. J. *Nano Lett.* **2001**, *1*, 155–158.
(12) Lalatonne, Y.; Richardi, J.; Pileni, M. P. *Nat. Mater.* **2004**, *3*, 121–125.
(13) Love, J. C.; Urbach, A. R.; Prentiss, M. G.; Whitesides, G. M. *J. Am. Chem. Soc.* **2003**, *125*, 12696–12697.
(14) Ahniyaz, A.; Sakamoto, Y.; Bergstrom, L. *Proc. Natl. Acad. Sci. U.S.A.* **2007**, *104*, 17570–17574.
(15) Ding, T.; Song, K.; Clays, K.; Tung, C.-H. *Adv. Mater.* **2009**, *21*, 1936–1940.
(16) de Gennes, P. G. *Rev. Mod. Phys.* **1992**, *64*, 645–648.
(17) Perro, A.; Reculusa, S.; Ravaine, S.; Bourgeat-Lami, E.; Duguet, E. *J. Mater. Chem* **2005**, *15*, 3745–3760.
(18) Nisisako, T.; Torii, T.; Takahashi, T.; Takizawa, Y. *Adv. Mater.* **2006**, *18*, 1152–1156.
(19) Kim, S.-H.; Jeon, S.-J.; Jeong, W. C.; Park, H. S.; Yang, S.-M. *Adv. Mater.* **2008**, *20*, 4129–4134.
(20) Roh, K. H.; Martin, D. C.; Lahann, J. *Nat. Mater.* **2005**, *4*, 759–763.
(21) Nie, Z.; Li, W.; Seo, M.; Xu, S.; Kumacheva, E. *J. Am. Chem. Soc.* **2006**, *128*, 9408–9412.
(22) Shepherd, R.; Conrad, J.; Rhodes, S.; Link, D.; Marquez, M.; Weitz, D.; Lewis, J. *Langmuir* **2006**, *22*, 8618–8622.

particles onto substrates to mask one hemisphere from a chemical or physical treatment.[17,23] Although these indirect techniques generate particles with high hemispheric feature uniformity, they suffer from reduced production rates and an inability to load chemical or biological payloads such as dyes, fluorophores, colloids or cells, limiting their uses in biomedical applications.

In particular, the generation of monodisperse, spherical particles with anisotropic superparamagnetic susceptibility and homogeneous biphasic geometry shows promise for many applications ranging from fundamental studies on self-assembly to the development of photonic crystals and drug delivery systems; yet, their synthesis have remained challenging. For example, recent efforts utilizing flame synthesis[24] and electrostatic[25] as well as magnetostatic[26] nanoparticle phase separation in polymeric microparticles have only succeeded in generating highly polydisperse particles characterized by ferromagnetic behavior and poorly defined Janus interfaces with particle-to-particle variation. Similarly, the synthesis of Janus particles using alginate chemistry is an alternative plagued by polydispersity,[27] an issue that complicates both the predictability and reproducibility of self-organized complex materials and their final effective properties. One solution to particle polydispersity involves evaporating a thin magnetic iron shell onto preexisting polystyrene spheres;[28] however, particles produced in this fashion are not bicompartmental and also lack superparamagnetic behavior, a requisite property for predictable rapid-response field-driven assembly and many biomedical applications such as detection in magnetic resonance imaging, separation, and drug delivery.[29] Thus, achieving efficient synthesis of monodisperse, bicompartmental and superparamagnetic Janus particles is of broad interest to many applications.

Here, we report the microfluidic synthesis and field-driven self-assembly of monodisperse, multifunctional Janus hydrogel particles with anisotropic superparamagnetic susceptibility and chemical composition. We have previously reported the synthesis of homogeneous nonspherical magnetic hydrogel microparticles.[30] Now, we aim to develop a particle based on the following design criteria: (a) the particle comprises biocompatible, antibiofouling polymer previously approved by the Food and Drug Administration (FDA) to facilitate future clinical implementation, (b) the particle assembles rapidly, anisotropically, and predictably in response to an external magnetic field, and (c) the particle exhibits multifunctionality via compartmentalization of varying chemistries (e.g., DNA, fluorophores), enabling differential surface modification or environmental responsiveness. By satisfying these criteria, these particles are ideal candidates for building three-dimensional hydrogel superstructures with chemically and magnetically tunable complexity for tissue engineering and sensing applications.

2. Experimental Section

2.1. Materials. In our microfluidic flow-focusing device, two streams of mineral oil (continuous phase) (Sigma Aldrich, St. Louis, MO) with 3% (v/v) ABIL EM 90 nonionic emulsifier (Degussa, Düsseldorf, Germany) sheared off droplets of two coflowing polymeric streams (dispersed phases), one containing UV-curable monomer and magnetic material M_m and one not containing magnetic material M_n.

In the magnetic characterization and self-assembly experiments, we used a mixture of (34% v/v) poly(ethylene glycol)−diacrylate (PEG-DA, Sigma Aldrich, St. Louis, MO, MW = 700, ρ = 1.12 g/mL, μ = 70 cP), (6% v/v) 2-hydroxy-2-methylpropiophenone (Darocur 1173, Sigma Aldrich, St. Louis, MO, MW = 164.2, ρ = 1.077 g/mL, μ = 25 cP), (2.4% v/v) glycerol (Mallinckrodt, Hazelwood, MO, MW = 92.1, ρ = 1.261 g/mL) and (57.6% v/v) deionized water as M_n; and (34% v/v) PEG-DA, (6% v/v) Darocur 1173, (25% v/v) water-based ferrofluid (EMG-508, Ferrotec, Bedford, NH, ρ = 1.07 g/mL, μ = 5 cP) and (35% v/v) deionized water as M_m.

In the microbead encapsulation experiments, we used a mixture of (34% v/v) PEG-DA, (6% v/v) Darocur 1173, (2.4% v/v) glycerol, (56.6% v/v) deionized water, (0.5% v/v) 4.5 μm Fluoresbrite YG carboxylate polystyrene microspheres (Polysciences, Inc.) and (0.5% v/v) 1.0 μm Fluoresbrite polychromatic red microspheres (Polysciences, Inc., Warrington, PA) as M_n; and (34% v/v) PEG-DA, (6% v/v) Darocur 1173, (25% v/v) EMG-508, (35% v/v) deionized water and (0.01 wt %) methacryloxyethyl thiocarbamoyl rhodamine B (Polysciences, Inc., Warrington, PA) as M_m.

In the DNA hybridization experiments, we used a mixture of (34% v/v) PEG-DA, (6% v/v) Darocur 1173, (2.4% v/v) glycerol, (57.6% v/v) TE buffer (10 mM tris(hydroxymethyl)-aminomethane, 1 mM ethylenediaminetetraacetic acid, pH = 8.0, Rockland Immunochemicals, Inc., Gilbertsville, PA) containing 0.01% v/v of 10 wt % sodium dodecyl sulfate (SDS, Sigma Aldrich, St. Louis, MO) and 50 μM DNA-Acrydite capture DNA (Integrated DNA Technologies, Coralville, IA) as M_n; and (34% v/v) PEG-DA, (6% v/v) Darocur 1173, (25% v/v) EMG-508 and (35% v/v) deionized water as M_m. The DNA probe was modified with a reactive Acrydite group and 18-carbon spacer: 5′-Acrydite-C18-ATA GCA GAT CAG CAG CCA GA-3′. The probe's complementary target DNA oligomer was modified with a Cy3 fluorophore (Integrated DNA Technologies, Coralville, IA) and suspended in 1 M hybridization buffer (TE buffer with 0.2 M NaCl (Mallinckrodt, Hazelwood, MO) and 0.5% SDS). All mineral oil, PEG-DA, and deionized water were filtered using a 0.2 μm sterile syringe filter prior to use.

2.2. Microfluidic Devices. We prepared silicon wafers containing positive-relief channels patterned in SU-8 photoresist (MicroChem Corp., Newton, MA). Following spin-coating of photoresist onto the surface of the wafers and a quick 65 °C prebake, we exposed the wafers with UV light shown through a transparency mask designed using AutoCAD 2009 (Autodesk, Inc., San Rafael, CA) and printed with 20000 dpi resolution at CAD/Art Services (Brandon, OR). Following a 95 °C postbake, we used a developer to remove any photoresist unexposed to UV.

Using soft lithography, we fabricated microfluidic devices by pouring a 10:1 ratio by weight mixture of poly(dimethylsiloxane) (PDMS, Sylgard 184, Dow Corning, Midland, MI) and curing agent (degassed for 30 min prior to wafer application) onto the patterned wafer at a depth of 5 mm. Then, we cured the PDMS for 8 h at 65 °C and subsequently sealed cut microchannels to a PDMS-coated glass slide. Briefly, glass slides were previously coated with a thin layer of PDMS and partially cured for 20−25 min at 65 °C. We cleaned microchannels with several washes of ethanol and deionized water under sonication and placed the dried PDMS onto the glass slides for contact sealing and an additional 1 h bake at 65 °C.

2.3. Photopolymerization Setup. We loaded solutions for microparticle synthesis into the microfluidic devices using 18-gauge stub adapters (Intramedic Luer-Stub Adapters, Becton, Dickinson and Company, Franklin Lakes, NJ) connected to rubber tubing (Tygon, Saint-Gobain SA, Courbevoie, France) to a common pressure source. We independently infused the polymeric and oil solutions into the channels by controlling the

(23) Paunov, V. N.; Cayre, O. J. *Adv. Mater.* **2004**, *16*, 788–791.
(24) Zhao, N.; Gao, M. *Adv. Mater.* **2009**, *21*, 184–187.
(25) Shah, R. K.; Kim, J.-W.; Weitz, D. A. *Adv. Mater.* **2009**, *21*, 1949–1953.
(26) Dyab, A. K. F.; Ozmen, M.; Ersoz, M.; Paunov, V. N. *J. Mater. Chem* **2009**, *19*, 3475–3481.
(27) Zhao, L. B.; Pan, L.; Zhang, K.; Guo, S. S.; Liu, W.; Wang, Y.; Chen, Y.; Zhao, X. Z.; Chan, H. L. W. *Lab Chip* **2009**, *9*, 2981–2986.
(28) Smoukov, S. K.; Gangwal, S.; Marquez, M.; Velev, O. D. *Soft Matter* **2009**, *5*, 1285–1292.
(29) Neuberger, T.; Schpf, B.; Hofmann, H.; Hofmann, M.; von Rechenberg, B. *J. Magn. Magn. Mater.* **2005**, *293*, 483–496.
(30) Hwang, D. K.; Dendukuri, D.; Doyle, P. S. *Lab Chip* **2008**, *8*, 1640–1647.

input pressure using type 100LR precision air pressure regulators (ControlAir, Inc., Amherst, NH) attached with a digital pressure gauge (DPG 100G, OMEGA Engineering, Inc., Stamford, CT, 0 to 103.4 kPa pressure range) and connected in series to a three-way solenoid valve (Bürkert, Ingelfingen, Germany, operated via computer using a script written in LabView (National Instruments, Austin, TX)) that allowed for switching between pressurized (3 psi, flow) and unpressurized (0 psi, no flow) operation states. We performed microfluidic-based particle synthesis and self-assembly studies using an Axiovert 200 (Carl Zeiss AG, Jena, Germany) inverted microscope connected to a 100 W HBO mercury lamp as the UV light source for particle photopolymerization. A wide-range excitation UV filter (11000v2:UV, Chroma, Rockingham, VT) selected UV light at the desired spectrum. To check process quality and throughput, movies of the synthesis process were recorded using a video tape recorder (DSR-25, Sony) using a CCD camera that captured images at the rate of 30 frames/second using an exposure of 1/1500 s. We used a Nikon D200 camera (DigitalSLR) to capture color images of Janus particle synthesis and self-assembly. Finally, we used scanning electron microscopy (SEM, JEOLJSM 6060) to examine the morphology of the Janus hydrogel particles.

2.4. Particle Recovery. Following synthesis, we recovered the particles from a collection reservoir at the terminus of the microfluidic channel by adding a (10% v/v) PEG-DA and (90% v/v) deionized water with 0.005% (v/v) Tergitol NP-10 (Sigma Aldrich, St. Louis, MO) (to prevent nonspecific sticking between the hydrogel particles and their containers) solution and withdrawing the solution and particles into a clean Eppendorf tube. We removed unreacted monomer and mineral oil from the suspension by rinsing with alternating solutions of 100% ethanol and 0.005% (v/v) Tergitol NP-10 solution, centrifuging the particle sample, and removing excess rinsing solution. This procedure was performed 10 times per particle batch.

2.5. Magnetic Characterization. We performed magnetic measurements of dried samples of Fe_3O_4 nanoparticles (EMG-508, Ferrotec, Bedford, NH), homogeneous magnetic hydrogels, and Janus hydrogels using a vibrating sample magnetometer (VSM, model DMS 1660) at a temperature of 300 K. Sample magnetization was recorded as the uniform magnetic field varied from −0.5 to 0.5 T. Before observing magnetic self-assembly, we dispersed suspensions of homogeneous and Janus hydrogel particles in a 0.005% (v/v) Tergitol NP-10 (Sigma Aldrich, St. Louis, MO) solution in a 5 mm × 5 mm × 5 mm PDMS reservoir sealed on top of a PDMS-coated glass slide. We evaluated the magnetic response of the particles at different values of fractional surface coverage, θ, where θ is defined as the ratio of the sum of the cross-sectional area of the particles to the reservoir area. To subject the particles to a uniform magnetic field, we placed the reservoir in an electromagnetic coil connected to a DC power supply (GPS-2303, GW Instek, Tucheng City, Taiwan). The induced magnetic fields were calibrated using a Gauss meter (SYPRIS, Orlando, FL) with an axial probe for normal induced fields and a transverse probe for planar induced fields.

2.6. Oligomer Hybridization. We mixed Janus particles with one hemisphere loaded with 50 μM DNA-Acrydite capture DNA (Integrated DNA Technologies, Coralville, IA) in a hybridization buffer (TE buffer with 0.2 M NaCl and 0.5% SDS) with 5 μM complementary target DNA oligomer modified with Cy3 fluorophore (Integrated DNA Technologies, Coralville, IA) and incubated at 37 °C with mild shaking for 30 min. We then rinsed the particles with a 0.005% (v/v) Tergitol NP-10 in TE buffer solution several times until there was no residual fluorescence in the particle solution.

3. Results and Discussion

First, we formed Janus droplets in a microfluidic flow-focusing device fabricated from poly(dimethyl-siloxane) (PDMS) using soft lithography (Figure 1A). In this device, two streams of mineral oil sheared off monodisperse droplets of two UV curable polymeric streams: one nonmagnetic poly(ethylene glycol)−diacrylate solution (PEG-DA, MW = 700, Sigma Aldrich, St. Louis, MO) and one PEG-DA solution containing magnetite (Fe_3O_4) nanoparticles (EMG-508, Ferrotec, Bedford, NH). Downstream of the flow-focusing region, a step-change in the channel height from 20 to 70 μm allowed the droplets to relax into spheres which were subsequently polymerized upon UV irradiation. We arranged a small rectangular piece of aluminum acting as a UV reflector above the microchannels in order to counteract particle shape deformation as a result of (a) heterogeneous UV energy distribution in a spherical particle and (b) reduction in UV dose due to strong iron oxide nanoparticle UV absorption. With our channel design, we generated 48 μm ± 1.8 μm-diameter (COV = 3.8%) Janus hydrogel spheres at a throughput of $\sim 10^5$ particles per hour by maintaining pressures of 0.7 psi at the dispersed phases/polymeric solutions inlet and 2.5 psi at the continuous phase/oil solution inlet. To minimize the mixing of Janus phases as a result of both asymmetric recirculatory flow and diffusion, previous efforts to synthesize Janus particles microfluidically required the use of viscous[19] or immiscible[21] phases, imposing limits on the particles' biocompatibility and chemical diversity. By positioning and adjusting the UV-exposed area (0−800 μm diameter) immediately downstream of the flow-focusing region where droplet formation occurs using an aperture in the inverted microscope, we successfully polymerized miscible Janus phases with up to 60% water content by volume without sacrificing the sharpness of the Janus interface (Figure 1B). We note that the particles in this figure have been reoriented by briefly exposing them to a weak magnetic field in order to highlight the particles' Janus interfaces. Furthermore, we confirmed with scanning electron microscopy (SEM) that our particles are spherical and highly uniform and retain their shape following drying (Figure 1C).

Next, we verified by vibrating sample magnetometry (VSM) that our synthesis procedure yields superparamagnetic hydrogel microparticles (zero coercivity, no hysteresis) (Figure 2). The initial degree of magnetization of a colloidal ferrofluid system in response to an applied magnetic field, the initial magnetic susceptibility χ_i, is given by an adaptation of the Langevin function for superparamagnetic magnetization

$$\chi_i = \frac{\mathbf{M}}{H} = \frac{\pi}{18}\frac{\phi\mu_0\mathbf{M}_d{}^2 d^3}{kT} \quad (1)$$

where $\mathbf{M}$ is the magnetization of a ferrofluid in the direction of an applied field, ϕ is the volume fraction of the magnetic solid in the ferrofluid, μ_0 is the magnetic permeability of free space, $\mathbf{M}_d$ is the saturation magnetization of the magnetic solid, H is the magnitude of the applied field, d is the diameter of a magnetic particle in the ferrofluid, k is the Boltzmann constant, and T is the temperature.[31] In this work, we determined the mass initial magnetic susceptibility $\chi_{i,mass}$ of dried hydrogels and dried nanoparticles by evaluating the slope of the magnetization curves ($\mathbf{M}$ versus H) at small values of applied field H (H = −0.02 to 0.02 T). On the other hand, the saturation magnetization of the ferrofluid at large applied fields is given by

$$\mathbf{M} = \phi\mathbf{M}_d\left(1 - \frac{6}{\pi}\frac{kT}{\mu_0\mathbf{M}_d d^3}\frac{1}{H}\right) \quad (2)$$

The quantity $\mathbf{M}_s = \phi\mathbf{M}_d$ represents the saturation magnetization of the ferrofluid. In this work, we determined the $\mathbf{M}_s$ of the dried

(31) Rosensweig, R. *Ferrohydrodynamics*; Cambridge University Press, Cambridge, U.K., 1985.

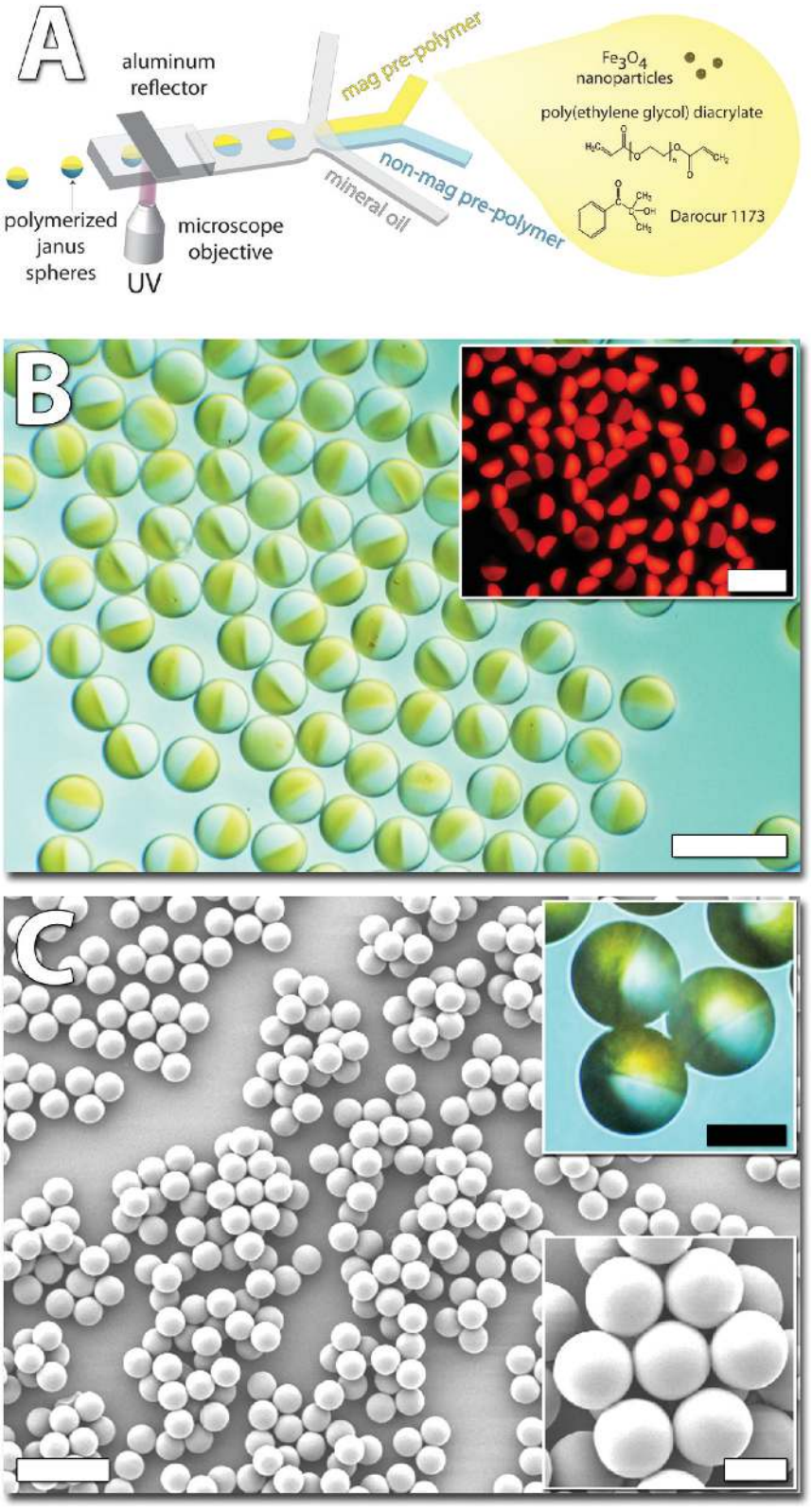

Figure 1. (A) Schematic of Janus particle synthesis in a flow-focusing microfluidic device. (B) DIC and corresponding fluorescent (insert) images of magnetic Janus particles generated from coflowing streams of polymer, one containing magnetic nanoparticles and the other containing rhodamine B. The scale bars are 100 μm wide. (C) SEM and DIC (upper right insert) images of dried Janus particles. The scale bars are 100 μm wide and 25 μm wide for the inserts.

hydrogels and dried nanoparticles from the intercept and slope of a linear fit of the magnetization **M** versus the inverse of the applied field H at large values of H (H = 0.2−0.5 T). Using a bulk magnetite (Fe_3O_4) saturation magnetization of $\mathbf{M}_d$ = 92 A m^2 kg^{-1},[32] the measured saturation magnetization value of the Janus particles at 300 K was 1.2 A m^2 kg^{-1}, while homogeneous magnetic hydrogel particle controls were determined to have a

(32) Yamaura, M.; Camilo, R.; Sampaio, L.; Macedo, M.; Nakamura, M.; Toma, H. *J. Magn. Magn. Mater.* **2004**, *279*, 210–217.

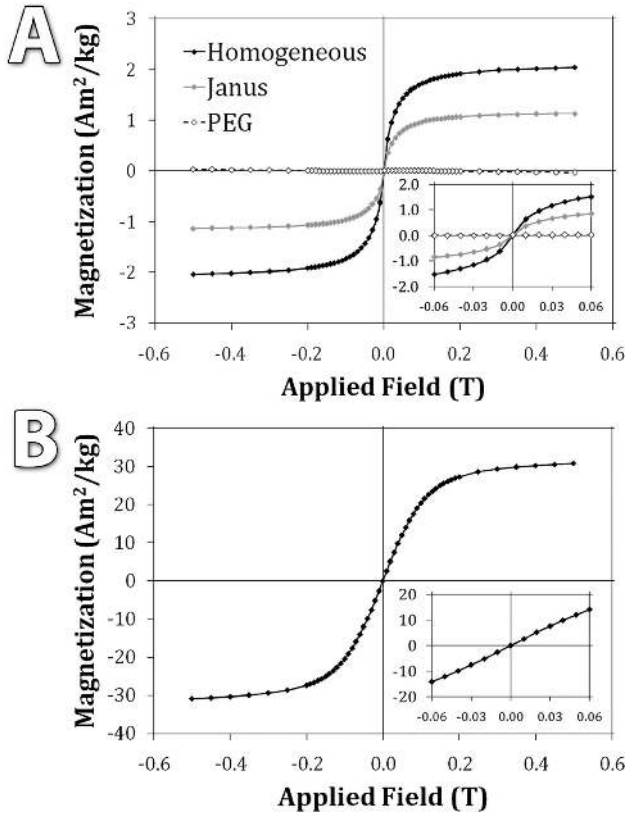

Figure 2. (A) Magnetization curves (T = 300 K) of dried homogeneous magnetic hydrogel particles (homogeneous, solid black curve), dried magnetic Janus particles (Janus, solid gray curve), and dried homogeneous nonmagnetic hydrogel particles (PEG, dotted black curve). (B) Magnetization curves (T = 300 K) of dried magnetite nanoparticles.

saturation magnetization value of 2.3 A m^2 kg^{-1}, approximately twice that of the Janus particles as expected. The mass initial magnetic susceptibility of the Janus particles was 3.6 $\times$ 10^{-5} m^3 kg^{-1}. In addition, the overall estimated Fe_3O_4 content of the Janus particle was 3.6%. Also, we determined that the Fe_3O_4 nanoparticles have a particle diameter of 7.8−9.8 nm, which is smaller than the manufacturer's specification (d = 10 nm). We note that the use of eq 2 will underestimate the nanoparticle's average diameter as the magnetic saturation approach is driven largely by the orientation of smaller iron oxide particles at large fields.[31] Furthermore, we verified that the nonmagnetic polymeric hemisphere in our Janus hydrogel particles has no magnetic susceptibility by evaluating samples of dried hydrogel spheres synthesized with a mixture of (34% v/v) PEG-DA, (6% v/v) photoinitiator (Darocur 1173), (2.4% v/v) glycerol, and (57.6% v/v) deionized water with VSM. The magnetic properties of the nanoparticles and hydrogels are summarized in Table 1.

By exposing the Janus particles to a weak magnetic field (2.0 $\pm$ 0.1 mT in-plane (parallel to substrate plane)) and then rotating the field, the particles acquired dipole moments and rotated freely such that their magnetic and nonmagnetic interfaces aligned with the direction of the field without physical translation along the field plane (Figure 3A−H, arrows indicating field direction). In the presence of an externally applied field, the orientation of the Janus particles is locally and precisely controlled, making them particularly useful for sorting applications as well as for microrheological probes[33] and magnetic imaging. While magnetic

(33) Khair, A. S.; Brady, J. F. *J. Rheol.* **2008**, *52*, 165–196.

Table 1. Magnetic Properties of Dried Fe_3O_4 Nanoparticles, Homogeneous Magnetic Hydrogels, and Janus Hydrogels

	Fe_3O_4 nanoparticle	homogeneous magnetic hydrogel	Janus hydrogel
nanoparticle diameter (nm)	7.8	9.6	9.8
Fe_3O_4 content (wt %)		6.9	3.6
initial magnetic susceptibility[a]	30.9 $\times$ 10^{-5}	7.0 $\times$ 10^{-5}	3.6 $\times$ 10^{-5}
saturation magnetization[b]	33.2	2.3	1.2

[a] $\chi_{i,mass}$ (m^3 kg^{-1}). [b] $\mathbf{M}_s$ (A m^2 kg^{-1}).

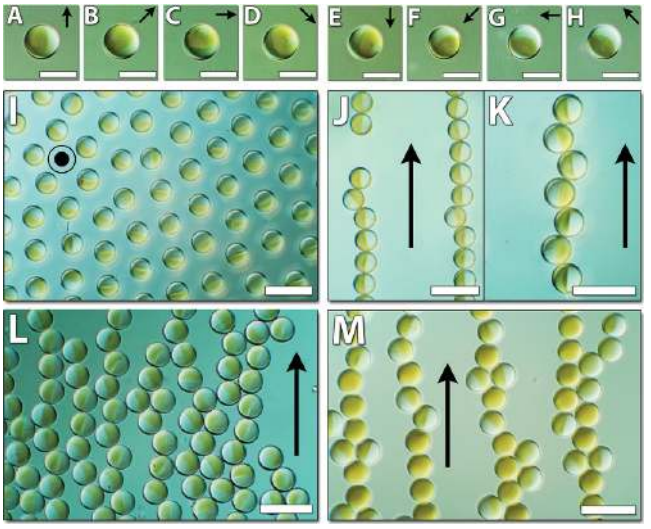

Figure 3. (A−H) DIC images of a Janus particle in response to a rotating magnetic field (2.0 $\pm$ 0.1 mT in-plane). The scale bars for panels A−H are 50 μm wide. (I−M) DIC images of self-assembling Janus spheres in chainlike structures in response to (I) out-of-plane (21.1 $\pm$ 0.1 mT) and (J,K) in-plane magnetic fields (14.7 $\pm$ 0.1 mT). (L) DIC image of self-assembling Janus spheres at high particle concentration. (M) DIC image of a self-assembling 1:1 mix of magnetically homogeneous and Janus particles. The scale bars for panels I−M are 100 μm wide.

micromanipulation of individual anisotropic particles could play a critical role in sorting and micromixing;[34] undoubtedly, the large-scale generation of novel and complex materials for fields ranging from tissue engineering to metamaterials rely on the organized, higher-order assemblies of the same particles. To demonstrate the Janus particles' potential for bottom-up assembly, we investigated their behavior in a 0.005% (v/v) aqueous Tergitol NP-10 solution in a PDMS reservoir in the presence of low-strength magnetic fields (14.7 $\pm$ 0.1 mT in-plane, 21.1 $\pm$ 0.1 mT out-of-plane (orthogonal to substrate plane)). By subjecting Janus particles dispersed in a reservoir at a fractional surface coverage θ smaller than 1 (where θ is defined as the ratio of the sum of the cross-sectional area of the particles to the reservoir area) to a homogeneous field perpendicular to the reservoir substrate, the particles repelled neighboring particles and self-assembled into a stationary, semiregular array with Janus interfaces visible (Figure 3I). At low fractional surface coverage $\theta \approx$ 0.05, Janus particles were observed to align in either straight (Figure 3J) or zigzag (Figure 3K) dipolar chainlike configurations

(34) Chen, C.-H.; Abate, A.; Lee, D.; Terentjev, E.; Weitz, D. *Adv. Mater.* **2009**, *21*, 3201–3204.

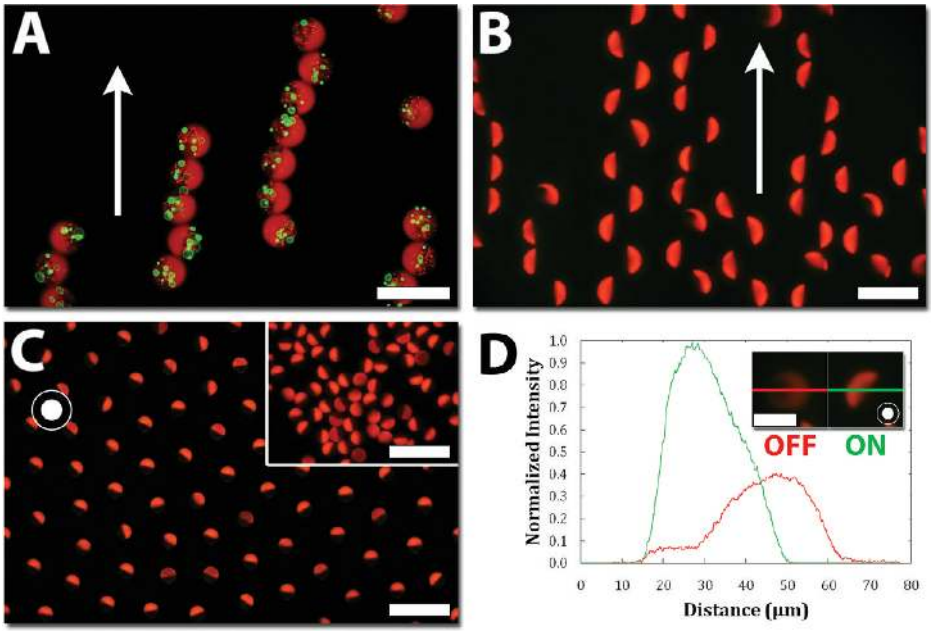

Figure 4. (A) Fluorescent image of self-assembling Janus particles containing 4.8 μm yellow-green and 1 μm red microspheres isolated in the nonmagnetic hemisphere. (B) Fluorescent image of self-assembling DNA-modified particles. The scale bars for panels A and B are 100 μm-wide. The applied fields in panels A and B are in-plane and 14.7 $\pm$ 0.1 mT in magnitude. (C) Fluorescent images of Janus particles self-arranging from an initially disordered state (inset) following the application of an out-of-plane field (10.0 $\pm$ 0.1 mT). The scale bars for panel C are 200 μm-wide. (D) Normalized fluorescence intensity of a line scan of a selected Janus particle before (OFF) and after (ON) field application (out-of-plane, 10.0 $\pm$ 0.1 mT). The scale bar for the inset is 50 μm wide.

in an in-plane external field. Interestingly, at higher θ's, meshlike superstructures formed as parallel chains zippered together (Figure 3L). The particle's anisotropic magnetic susceptibility permits one hemisphere to interact with satellite particles or nearby chains while preserving the chain's symmetry in a lateral field. In a low θ, 1:1 blend with homogeneous magnetic particles, Janus particles introduced defects and disrupted chain symmetries as they incorporated into the sides of chains (Figure 3M). Such behavior suggests that the complexity of constructs derived from bottom-up assembly can be modulated with particle concentration and composition in addition to field type.

The ability to precisely control the spatial distribution of biological payloads in a particle is another route for generating complexity in tissue engineering and finds use in potential drug delivery or cell mimicry systems.[35] As a proof of principle, we then successfully copolymerized the fluorophore methacryloxyethyl thiocarbamoyl rhodamine B as a model small molecule drug in the magnetic hemisphere and two fluorescent microbeads (one being green [4.8 μm-diameter], the other being red [1 μm-diameter] under UV) as model cells in the nonmagnetic hemisphere of the hydrogels (Figure 4A). Likewise, selective surface functionalization can play a critical role in chemical detection schemes for bioanalytical applications and can enable an additional parameter for the fine-tuning of controlled assembly of three-dimensional hydrogel structures. Accordingly, we demonstrated the utility of functionalized Janus particles for DNA detection by synthesizing particles with one hemisphere loaded with an acrylate-modified DNA probe (Integrated DNA Technologies) at 50 μM. After 30 min of incubation with Cy3-labeled complementary target at 5 μM in a hybridization buffer (TE buffer with 0.2 M NaCl and 0.5% w/v SDS), we were able to show selective capture on one-half of the particles as indicated by fluorescence microscopy (Figure 4B).

While the unambiguous identification of signal can be achieved easily from a single functionalized probe particle in a high-contrast environment during a biomedical imaging experiment or bioassay, signal detection becomes more challenging at both higher particle concentration and sample amount. The ability of multifunctional superparamagnetic Janus particles to enhance optical contrast by (a) simultaneously coding two chemistries per particle for differential analysis in a single step during synthesis and (b) quickly self-organizing into fixed and regular geometric patterns in response to an external magnetic field are therefore highly interesting for developing new approaches to monitoring assembled structures in response to external stimuli. To illustrate the potential of the Janus particles for generating optical contrast, we loaded Janus particles previously functionalized on one hemisphere with a fluorophor and an optically inert compound on the other hemisphere as a negative signal control into a PDMS reservoir (Figure 4C). Upon the application of an external magnetic field (10.0 $\pm$ 0.1 mT, out-of-plane), particles—initially dispersed with the optically active hemisphere obscured or confounded by a neighboring particle—arranged themselves into quasi-periodic arrays with both functionalized and control hemispheres in clear view. Figure 4D illustrates the signal enhancement in a close-up horizontal fluorescence intensity scan of an individual particle with an acrylate-modified DNA probe hybridized to the hemisphere containing complementary target DNA. Following magnetic field application, the peak normalized fluorescence intensity of the Janus particle increased 2.5-fold in the region of the functionalized hemisphere and dropped to essentially zero in the corresponding control region. Similarly, the total integrated fluorescence intensity of the particle increased over 60% in the presence of a magnetic field. Such responsiveness and optical enhancement capabilities indicate that these particles could be particularly useful for novel sensing applications like the miniaturization of dot blot analysis.[36]

(35) Mitragotri, S.; Lahann, J. *Nat. Mater.* **2009**, *8*, 15–23.

(36) Wright, S. F.; Morton, J. B. *Appl. Environ. Microbiol.* **1989**, *55*, 761–763.

4. Conclusions

We report the microfluidic synthesis of spherical Janus hydrogel particles with superparamagnetic properties and chemical anisotropy and their two-dimensional self-assembly into stable chainlike microstructures under an external magnetic field. To our knowledge, this work represents the first report of (a) the synthesis of a uniform superparamagnetic Janus particle and (b) the demonstration of bottom-up, field-driven assembly of hydrogels with controllable spatial distribution of biochemical payloads. Although these biocompatible Janus particles find immediate use in tissue engineering, their ability to self-assemble with tunable anisotropic configurations make them an intriguing material for several exciting areas of research such as photonic crystals, novel microelectronic architecture, and sensing. With controllable compositions, these multifunctional microparticles offer a promising building block for engineering complex mesoscale assemblies with heterogeneous geometries and biophysicochemical properties.

Acknowledgment. We gratefully acknowledge the support of the Singapore−MIT Alliance (SMA-II, CPE Program) and the Guggenheim Foundation for this project. The authors thank D.C. Pregibon for discussions concerning DNA hybridization and H.S. Kim for his assistance with vibrating sample magnetometry.